Observations of Seiche Forcing and Amplification in Three Small Harbors

By Michele Okihiro[1] and R. T. Guza[2]

ABSTRACT: Extensive field observations are used to characterize seiches (periods 0.5–30 min) in three small harbors with similar surface areas ($\sim$1 km^2), water depths (5–12 m), and swell wave climates. On the continental shelf just offshore of each harbor mouth, the energy levels of waves in the infragravity frequency band 0.002–0.03 Hz (periods 0.5–10 min) vary by more than a factor of 200 in response to comparably large variations in swell energy levels. Energy levels in this swell-driven frequency band also vary (less dramatically) in response to changes in the swell frequency and with tidal stage. Motions at longer seiche periods (10–30 min) are primarily driven by meteorological and other processes (a tsunami-generated seiche is described). As has often been observed, the amplification of seiche energy within each harbor basin (relative to energy in the same frequency band outside the harbor) varies as a function of seiche frequency, and is largest at the frequency of the lowest resonant harbor mode (i.e., the Helmholtz or grave mode). At all three harbors, the average amplification of the grave mode decreases (by at least a factor of 2) with increasing seiche energy, a trend consistent with a nonlinear dissipation mechanism such as flow separation in the harbor mouth or sidewall and bottom friction.

INTRODUCTION

Seiches in small harbors are standing long waves at the periods of the harbor normal modes, typically in the period range 0.5–30 min. The seiche band in small harbors includes both swell-driven infragravity waves [nominally 0.5–10 min periods, e.g., Munk (1949)] and shelf waves [10–30 min periods, e.g., Munk et al. (1956)]. Energy at the resonant periods is amplified within the harbor, relative to outside the harbor, whereas motions within the harbor at other periods are suppressed. When sufficiently energetic, seiches cause costly delays in loading operations and damage ships and shoreside facilities. Although numerical and laboratory studies of harbor seiche exist, their utility has been limited because energy levels in the seiche frequency band outside natural harbors (which directly drive seiches within the harbor) are generally unknown, and the damping mechanisms that apparently can limit seiche amplification inside harbors are poorly understood.

Most previous field data used to study harbor seiches have been restricted to a relatively small range of conditions sampled during short deployments. Additionally, the length of individual time series was sometimes insufficient to resolve the frequencies of the seiche modes, and spatial coverage of the sensors was often sparse. In some cases, the offshore observations needed to calculate seiche amplifications were absent or collected far from the harbor mouth. Recently more comprehensive data sets have been collected at three small harbors in California and Hawaii. Seiche at one of these sites (Barbers Point, Hawaii) is discussed in Okihiro et al. (1993) (hereafter OGS). Observations of seiche in these harbors are compared and contrasted here in order to assess the generality of the Barbers Point results.

It has been shown theoretically and in laboratory experiments that low-frequency bound waves (associated with groups of swell impinging on a harbor mouth) can drive harbor seiche at the group frequency (Bowers 1977; Mei and Agnon 1989; Wu and Liu 1990). However, observations (including

sites both near and far from harbors) on the continental shelf in depths comparable to the depths of small harbors [i.e., $O(10$ m)] show that free waves usually contribute the bulk of the energy in the swell-driven infragravity band (e.g., 0.5–10 min periods) (Okihiro et al. 1992; Elgar et al. 1992; Bowers 1992; Herbers et al. 1995a). Bound and free infragravity energy levels on the shelf are similar only when swell energy levels are very high. Free infragravity energy levels are not predictable from the swell properties because their generation and subsequent propagation are not understood. Recent observations show that free infragravity waves are generated in and radiated from very shallow water and subsequently refractively trapped on the shelf (Elgar et al. 1994; Herbers et al. 1994, and 1995b). Thus, although infragravity waves on the shelf adjacent to the harbors are likely nonlinearly generated on nearby beaches, nonlinear generation effects (e.g., bound infragravity waves) may be negligible in the harbor (Wu and Liu 1990) and near the harbor mouth.

OGS found qualitatively good agreement between seiche amplifications (e.g., the ratio of energies inside and outside the harbor at the same frequency) observed at Barbers Point and the predictions of a linear, inviscid numerical model. This confirms the underlying model assumption that seiche in small harbors can be approximated as the linear response of the semi-enclosed basin to free long waves outside the harbor. If the seiche were undamped, the amplification at any particular frequency would be constant. However, OGS observed a decrease in amplification with increasing swell and seiche energy, consistent with increased dissipation. These previous results motivate the approach adopted here, where we consider first the motions at seiche frequencies both outside and inside the harbors, and then the seiche amplification (as a function of both seiche frequency and swell and infragravity energy levels).

FIELD SITES AND MEASUREMENTS

Bottom-mounted pressure sensors were deployed at three small harbors with similar [$O(1$ km^2)] surface areas and depths (Fig. 1). Barbers Point and Kahului Harbors in Hawaii are commercial harbors and Oceanside Harbor in California is primarily used by recreational boaters.

Barbers Point Harbor is located on a straight coastline on the southwest side of the island of Oahu, where offshore bottom contours are relatively parallel and steep. The main harbor basin is approximately 12 m deep and there is a 1 km long dredged entrance channel [Fig. 1(a)]. A shallow (4–5 m depth)

[1]Ctr. for Coast. Studies, Scripps Instn. of Oceanography, Univ. of California at San Diego, 9500 Gilman Dr., La Jolla, CA 92093-0209.

[2]Ctr. for Coast. Studies, Scripps Instn. of Oceanography, Univ. of California at San Diego, 9500 Gilman Dr., La Jolla, CA.
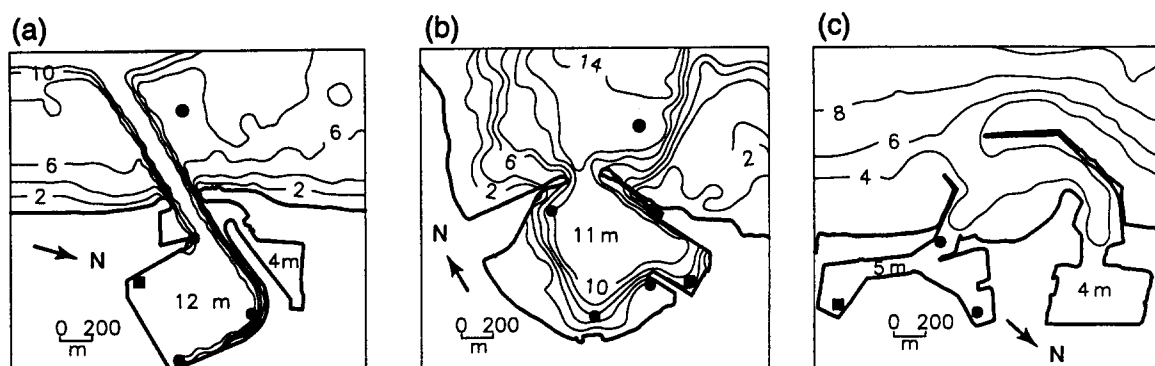
FIG. 1. Instrument Positions (Solid Circles and Squares) and Water Depths (m)

small boat marina connects to the deep-draft harbor through a channel near the main harbor entrance. Four sensors were located in the main harbor basin and one about 0.5 km offshore in 8.5 m depth [Fig. 1(a)].

Kahului harbor is situated at the apex of a large V-shaped bay formed by an indentation on the north shore of the island of Maui [Fig. 1(b)]. The offshore bathymetry at this site is complicated. East of the harbor entrance, shallow areas (<3 m depth) extend 1–2 km offshore, whereas to the west the bottom slope is steeper and relatively constant. Directly offshore of the harbor entrance the depth is 10–12 m. The 11 m deep operational portion of the harbor is surrounded by shallower regions along the western and southern perimeter. A 200 m wide entrance channel faces northward and is bounded by two rubble-mound breakwaters. Four sensors within the harbor were in mean depths between 2 and 10 m. The sensor outside the harbor is about 0.4 km offshore of the channel entrance in 14.5 m depth.

Oceanside Harbor, located on a relatively straight portion of the Southern California coastline, is adjacent to mildly sloping beaches. Breakwaters border both sides of the harbor entrance [Fig. 1(c)] and harbor depths range from 2 to 8 m. Sensors were located in depths of 5–8 m at three harbor sites and at about 2 km southeast of the harbor entrance in 11 m depth.

Time series records of 2.3 h duration sampled at between 0.5 and 2.0 Hz were collected between four and eight times a day at each site. The data discussed here are from October 1989 to March 1990 (479 records) at Barbers Point, October 1993 to January 1995 (3294 records) at Kahului, and May 1992 to December 1993 (3766 records) at Oceanside. Data from all sensors were analyzed. Results from harbor sensors discussed extensively in the text (denoted by square symbols in Fig. 1) are in depths of 11 m (south corner at Barbers Point), 8 m (eastern sensor at Kahului), and 5.6 m (eastern sensor at Oceanside). Each 2.3 h time series was detrended to remove tides. Fourier coefficients of pressure were converted to sea surface elevation spectra using linear theory.

This study is focused on the significantly amplified seiches that occur at frequencies below the incident sea-swell band. The 0.03 Hz upper limit of the selected seiche band (0.0005–0.03 Hz) is in a spectral valley in the sea surface elevation spectra of many offshore records [e.g., Fig. 5(b)] and was chosen to separate wind-generated long-period Pacific swell from lower frequency motions that are not forced by the wind. The 0.0005 Hz low-frequency limit (corresponding to a period of about 30 min) is determined by the frequency resolution of the data records, and is lower than the frequency of the grave mode (the lowest resonant frequency) of each of these harbors.

SEICHE FORCING AND RESPONSE

Seiche Energy Spectra

Average (over all data) spectra at seiche frequencies (0.0005–0.03 Hz) at the offshore and selected harbor sites are

shown in Figs. 2(a and b) (spectra from other harbor gauges are similar). The seiche-frequency spectra $E_{SEICHE}(f)$ offshore (outside) of Barbers Point harbor is approximately white [Fig. 2(a)]. However, outside of Oceanside and (especially) Kahului harbors, the energy levels at very low seiche frequencies are relatively elevated. On average 14% and 57% (respectively) of the total seiche-frequency energy is at frequencies less than 0.002 Hz, compared with only 7% of the offshore energy at Barbers Point. In contrast to the relatively smooth energy spectra observed offshore, seiche spectra in the harbors are characterized by peaks corresponding to the frequencies of resonant standing waves [Fig. 2(b)].

The average cumulative energy E_{SEICHE} outside the harbors increases smoothly [Fig. 2(c)] in contrast to the step increases inside the harbor at the resonant frequencies [Fig. 2(d)]. Energy at frequencies below 0.002 Hz on average accounts for about 70% of the total seiche-band energy inside Kahului and Oceanside harbors but only 40% at Barbers Point.

Effect of Swell Energy

At frequencies above ~0.03 Hz the offshore spectra at all three sites are typically [e.g., Fig. 5(b)] dominated by wind-generated swell. The correlations r between the log of seiche spectral levels $E_{SEICHE}(f)$ outside the harbors in narrow 0.0005 Hz frequency bands and the log of the total offshore swell energy (E_{SWELL}, the energy integrated over the 0.03–0.125 Hz swell band) vary with frequency and are relatively high in the infragravity frequency range from 0.002 to 0.03 Hz, as has been noted at many shelf sites [e.g., Munk (1949); Middleton et al. (1987); Nelson et al. (1988); Elgar et al. (1992); Herbers et al. (1995a)]. Similar correlations are observed between E_{SWELL} and seiche-frequency energy within the harbor [compare Fig. 2(e) with Fig. 2(f)].

The seiche-frequency band (0.0005–0.03 Hz) was split into three broad bands roughly corresponding to the degree of correlation with offshore swell [Fig. 2(e and f)]. Energy in the lowest frequency band (0.0005–0.002 Hz) is weakly correlated with E_{SWELL}. Energy in the second frequency or midfrequency band (0.002–0.01 Hz) is highly correlated with E_{SWELL}. Correlations in the third or high-frequency band (0.01–0.03 Hz) are high at Kahului and Barbers Point and somewhat lower at Oceanside [Fig. 2(f)].

The correlations with E_{SWELL} decrease substantially for frequencies less than about 0.002 Hz. Internal and shelf waves [e.g., Giese et al. (1990)], tsunamis [e.g., Wilson (1971)], and meteorological or atmospheric disturbances [e.g., Gomis et al. (1993)] excite harbor seiche oscillations at these periods of $O(10$ min) or longer. These not-driven-by-swell motions include the grave mode of the harbors, characterized by approximately equal energy and zero phase lags at locations in the harbor interior (e.g., Fig. 10 in OGS for examples of the spatial patterns at Barbers Point). The frequency of the amplified
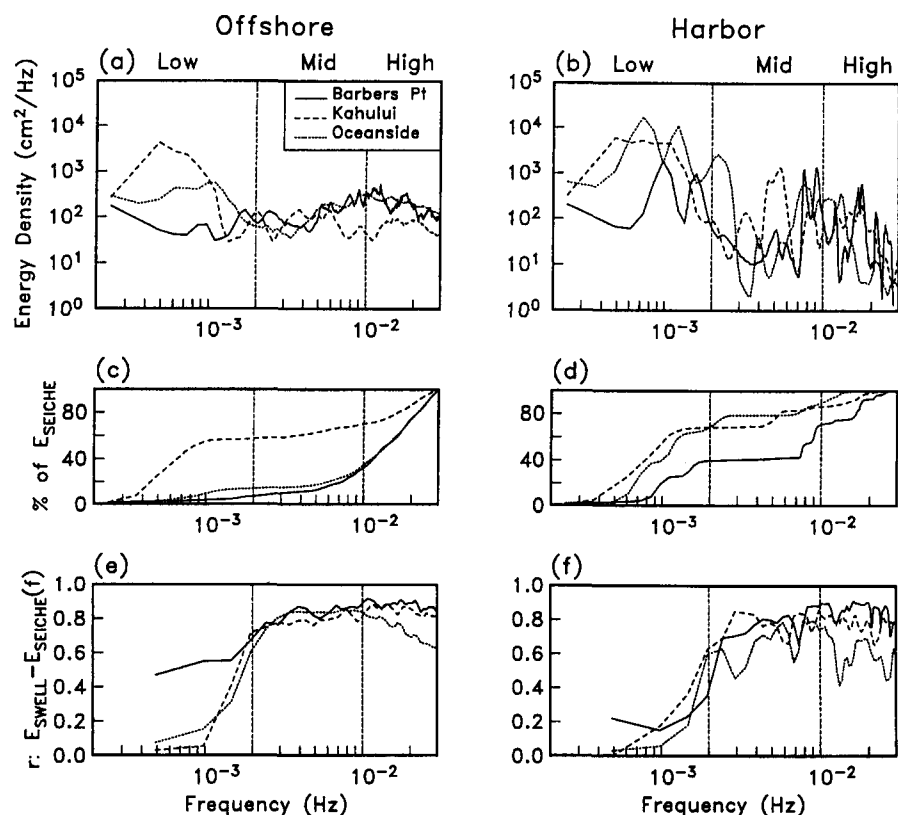
FIG. 2. (a, b) Average Observed Sea Surface Elevation Spectra; (c, d) Cumulative Percentage of Total Seiche-Frequency Energy; and (e, f) Correlations (r) between Total Offshore Swell Energy E_{SWELL} and Seiche-Frequency Energy $E_{SEICHE}(f)$ in Narrow (0.0005 Hz width) Frequency Bands outside (a, c, e) and within (b, d, f) Harbors as Function of Seiche Frequency
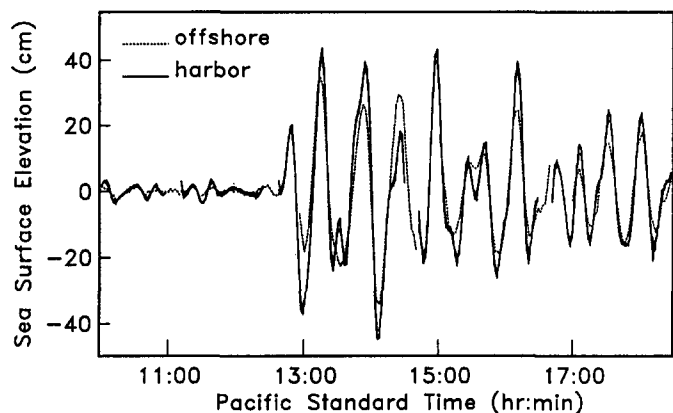

FIG. 3. Low Pass Filtered (2 min average) Sea Surface Elevation Time Series (Pacific Standard Time) on Oct. 4, 1994 Off Shore of and at Four Sites within Kahului Harbor

grave mode depends on the harbor depth and geometry and ranges from ~0.001 Hz at Barbers Point to ~0.0007 Hz in the shallower harbor at Oceanside [Fig. 2(b)]. (The energy peak expected at the roughly 0.001 Hz grave mode inside Kahului harbor is broad [Fig. 2(b)] because the offshore energy levels rise at frequencies below 0.001 Hz [Fig. 2(a)]. Atmospheric pressure disturbances were shown to sometimes excite the grave mode ($f \sim 0.001$ Hz) at Barbers Point harbor (Fig. 4 in OGS). At Kahului, tsunami waves generated by the October 4, 1994 Kuril Island earthquake resulted in significant [$O(1\text{ m})$ height] oscillations with ~30 min period (frequency 0.0005 Hz) both inside and outside the harbor. The motions within and near the harbor are in phase with similar amplitudes (Fig. 3). The tsunami data were excluded from, or are shown separately in (by triangles), the figures below.

Offshore energy integrated over the lowest and highest

seiche-frequency subbands, shown as a function of E_{SWELL} in Fig. 4, are generally consistent with the frequency dependent correlations [Fig. 2(e)]. The seiche energy is integrated over the low-frequency (0.0005–0.002 Hz) [Fig. 4(a–c)] and high frequency (0.01–0.03 Hz) [Fig. 4(d–f)] subbands. The highest frequency band [Fig. 4(d–f)] has a much stronger dependence on E_{SWELL} than the lowest band [compare Fig. 4(a–c) with 4(d–f)], although very energetic swell can excite detectable energy in the grave-mode-containing lowest frequency band at all three sites, especially at Barbers Point [Fig. 4(a)], where ambient energy levels in this frequency band are lower than at other sites. The triangles in Fig. 4(b) denote data from Oct. 4–6, 1994 at Kahului collected during the arrival of remotely generated tsunami waves (Fig. 3).

Effect of Swell Frequency

Infragravity energy levels at the same offshore site with similar E_{SWELL} can vary by more than a factor of 10, as illustrated in Fig. 4 for the low- and high-frequency bands at all sites, and in Fig. 5(a) for the seiche midfrequency range 0.002–0.01 Hz at Kahului. Some of this variation is associated with the sensitivity of infragravity wave generation to the swell frequency [e.g., Middleton et al. (1987); Okihiro et al. (1992); and Elgar et al. (1992) and references therein]. For example sea surface elevation spectra from two energetic swell events measured at the Kahului offshore sensor [Fig. 5(b)] have similar energy in the swell frequency band (0.03–0.125 Hz) but the long-period [$O(20\text{ s})$] swell waves on Jan 5, 1995 [Fig. 5(a,b)] were associated with about a factor of 10 more infragravity energy than on Nov. 26, 1993 [Fig. 5(a,b)], when the swell peak period was about 10 s. As in the example case [Fig. 5(b)], the dependence on swell frequency is generally stronger in the midfrequency seiche band than in the other seiche bands.
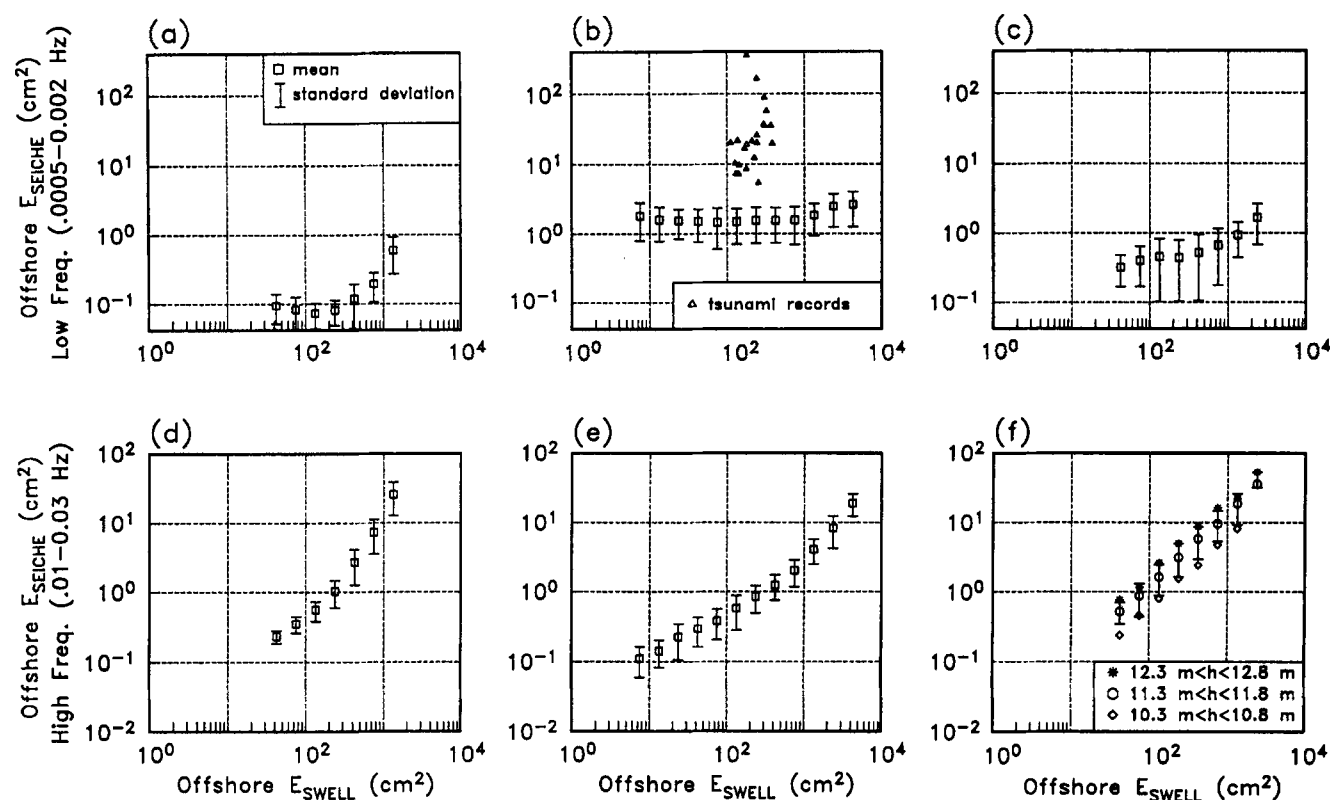
FIG. 4. Offshore Seiche Energy E_{SEICHE} versus Total Offshore Swell Energy E_{SWELL} over Two Frequency Subbands: (a) Barbers Point, Low Frequency; (b) Kahului, Low Frequency; (c) Oceanside, Low Frequency; (d) Barbers Point, High Frequency; (e) Kahului, High Frequency; (f) Oceanside, High Frequency

Tidal Modulation

Scatter in E_{SEICHE} at fixed E_{SWELL} is also associated with tidal fluctuations (Okihiro and Guza 1995). At Oceanside (tidal range $\sim$2.5 m), infragravity waves in the highest frequency subband (0.01–0.03 Hz) are factors of 5 to 10 times more energetic at high tide than during low tide both inside and offshore of the harbor (Fig. 6). The resonant frequencies in the harbor are also modulated, likely because of tidal changes in the harbor depths. The solid and dashed lines in Fig. 7(c) are for data at high and low tide, respectively. Correlations between E_{SWELL} and $E_{SEICHE}(f)$ are higher when records are separated by tidal stage [see Fig. 4(f)]. Tidal modulation of infragravity energy and shifts in the resonant frequencies also occurs at Barbers Point and Kahului (not shown), but are smaller probably because of the smaller tidal range ($\sim$1 m) at these mid–Pacific Ocean sites.

Harbor Amplification

The response of the harbors to forcing by waves outside the harbor is quantified here as the amplification, the ratio of smoothed power spectra (based on 2.3 h long records) inside to outside the harbors. Amplifications averaged over all records at each site are shown in Fig. 7 as a function of frequency. The 0.00024 Hz spectral bandwidth of the amplification spectra is coarse, particularly for resolving the lowest frequency modes ($f < 0.002$ Hz), but increasing the frequency resolution would further reduce the already low degrees of freedom [$O(6)$] of the power spectra used to estimate the amplification for each run. Over most of the infragravity frequency band, the offshore power spectra are white [Fig. 2(a)] and the shapes of the amplification spectra (Fig. 7) are due primarily to the harbor response. However, (spuriously) high amplifications can occur at frequencies corresponding to standing waves with nodes near the location of the offshore sensor. The effects of

nodal structure are reduced by basing amplifications on energies integrated over wider frequency bands.

Mean amplifications for the grave-mode-containing band ($f < 0.002$ Hz) and an additional higher frequency swell-driven mode (shown by the shaded bands in Fig. 7) are shown for each harbor as a function of offshore E_{SWELL} and offshore E_{SEICHE} in Figs. 8 and 9, respectively. At Barbers Point amplifications in the grave-mode frequency band systematically decrease (from 10 to about 3) with both increasing swell and increasing seiche energy [Figs. 8(a) and 9(a), respectively]. At higher frequencies the seiche mode amplifications are smaller [$O(1-5)$] and not sensitive to E_{SWELL} or E_{SEICHE} [Figs. 8(d) and 9(d)]. OGS attributed this amplification variation of the grave mode to nonlinear dissipation, which becomes increasingly important when waves are energetic. The most highly amplified modes are expected to be most affected by dissipation [e.g., Ito (1970); Murakami and Noguchi (1977); Kostense (1986); among others], as is observed [compare Figs. 8(a and d)].

At Kahului and Oceanside, the grave-mode amplification is approximately independent of swell energy [Figs. 8(b) and 8(c)] but decreases with increasing seiche energy [Figs. 9(b) and 9(c)]. [The triangles in Figs. 8(b) and 9(b) denote tsunami data.] The decrease in seiche amplification with increasing grave-mode energy [observed at all three harbors, Figs. 9(a–c)] is consistent with nonlinear damping associated with both flow separation in the entrance [e.g., Ito (1970); Unluata and Mei (1975)] and nonlinear side-wall and bottom friction [e.g., Kostense (1986)]. The dependence of the amplification on E_{SWELL} and E_{SEICHE} is similar to Figs. 8 and 9 for all sensors in each harbor. The lack of a dependence of grave-mode amplification on swell energy at Oceanside and Kahului [Figs. 8(b) and 8(c)] is somewhat surprising if (as is often assumed) energy losses are both nonlinear and concentrated near the harbor mouth. In this case, a dependence of seiche amplification on swell energy
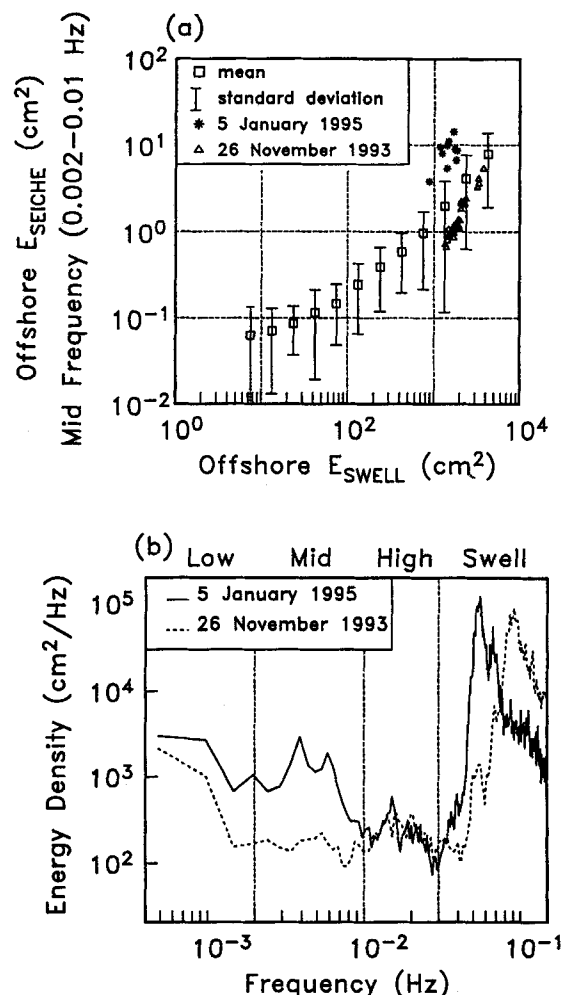
FIG. 5. (a) Offshore Energy Integrated over Seiche-Frequency Midband 0.002–0.01 Hz E_{SEICHE} as Function of Total Offshore Swell Energy E_{SWELL} at Kahului; (b) Sea Surface Elevation Spectra at Kahului Offshore Sensor
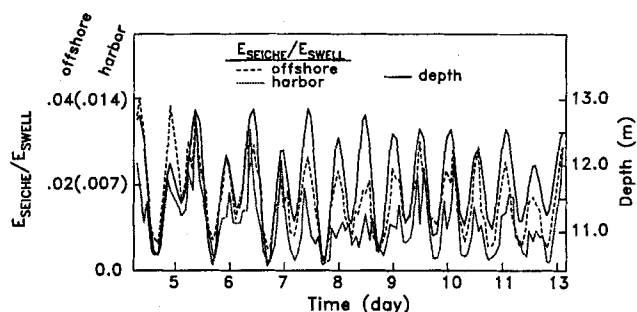

FIG. 6. Time Series of Offshore Depth and Offshore and Harbor High-Frequency E_{SEICHE} Normalized by Offshore E_{SWELL} at Oceanside for Feb. 4–13, 1993

levels is expected because swell orbital motions are usually larger than the seiche-induced velocities near the mouth and presumably contribute significantly to seiche damping. It may be that the dissipation at Kahului and Oceanside is occurring primarily at the bottom and side walls well within the harbor, where swell energies are relatively small. Ongoing numerical modeling is aimed at better understanding dissipative processes. Finally, note that although the mean amplifications of the grave-mode band clearly vary with E_{SEICHE}, there is a great deal of scatter in the amplifications at any particular value of E_{SEICHE} (Fig. 9). Some scatter is statistical, but other factors, such as tide-induced changes in the resonant frequencies and variations in the directional properties of infragravity waves

outside the harbor, likely also contribute to the scatter. In any event, the result that the average amplification of the grave mode depends on seiche energy at all three sites [Fig. 9(a–c)], but at Oceanside and Kahului is approximately independent of swell energy [in contrast to Barber Point, Figs. 8(a–c)], may provide useful guidance for future efforts to model seiche damping.

Seiche energy levels at all instrumented harbor locations (Fig. 1) are shown in Fig. 10 for the combined mid- and high-frequency (0.002–0.03 Hz) swell-driven band and the low-frequency (0.0005–0.002 Hz) not-swell-driven band. The solid symbols correspond to the harbor sensors discussed throughout the text and open symbols indicate the other harbor sensors (Fig. 1). Nearly equal seiche energy levels at sensors within the harbors appear as overlapping symbols. Differences between sensors in the same harbor are expected, owing to the spatial variation of seiche energy (e.g., nodes and antinodes). Note that despite these differences in detail, the trends for the particular harbor sensors considered earlier are observed for all harbor sensors (compare open and filled symbols). When the offshore swell (E_{SWELL}) is low, harbor seiche is dominated by energy in the low-frequency, grave-mode-containing band (<0.002 Hz); whereas higher frequency swell-driven seiches (>0.002 Hz) dominate when E_{SWELL} is high. The dependence of swell-driven seiche energy on E_{SWELL} is similar at all three sites and significant seiche wave heights reach 20–30 cm when significant swell heights exceed about 200 cm. (Significant heights are defined as four times the square root of the energy.) At the grave-mode frequencies, the amplifications are higher at Barbers Point and Oceanside than at Kahului [Figs. 8(a–c)], but because of differences in energy levels outside the harbors [Fig. 2(a)], the harbor seiche energy levels are
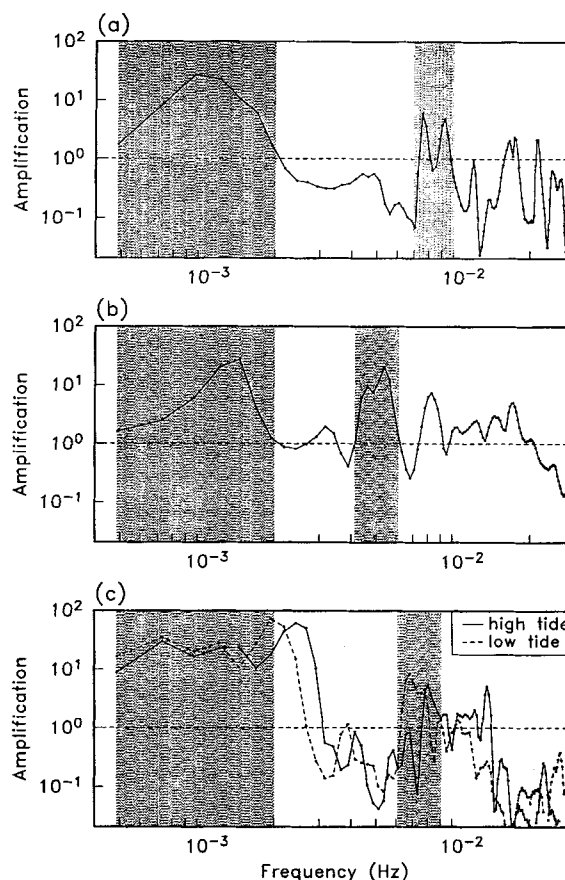

FIG. 7. Average Harbor Seiche Energy Amplification Spectra (Relative to Offshore): (a) Barbers Point; (b) Kahului; (c) Oceanside
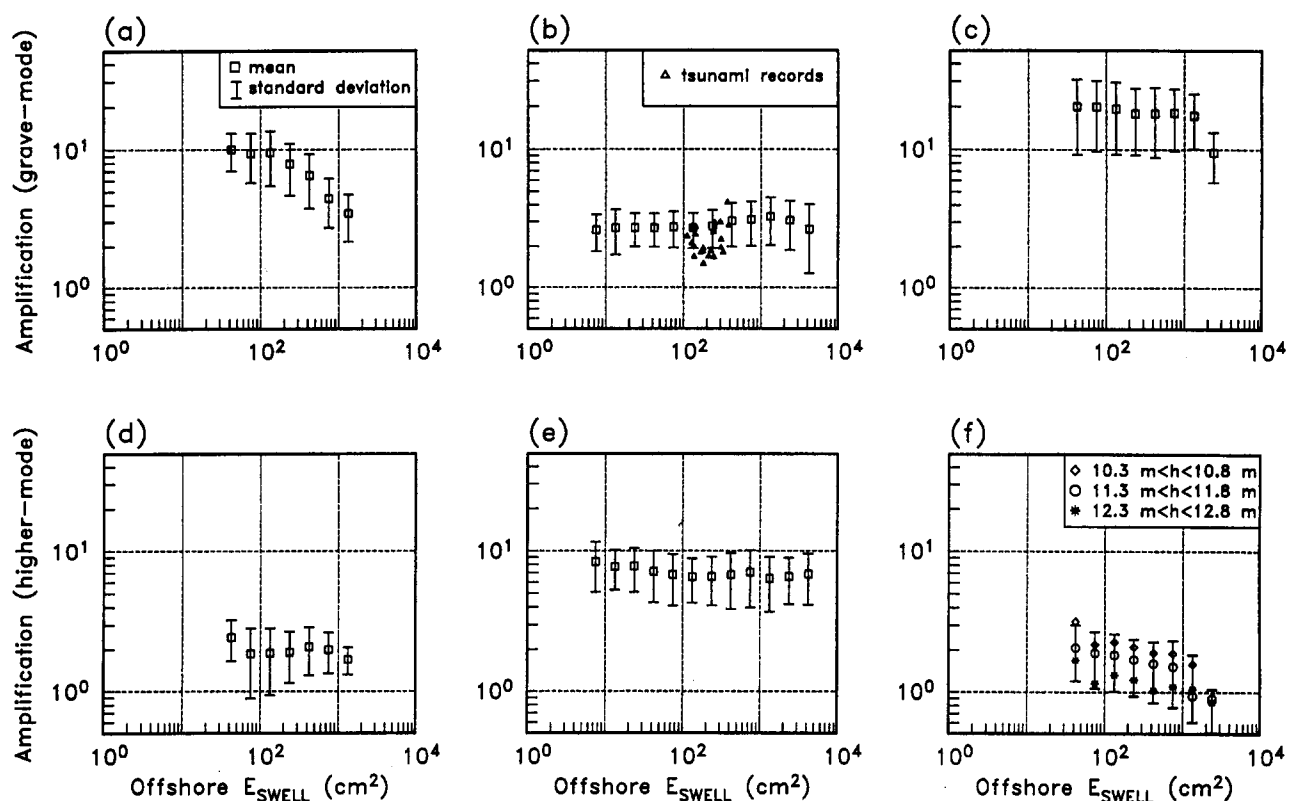
FIG. 8. Ratios of E_{SEICHE} within and Offshore of Harbors at (a–c) Grave Mode and (d–f) next Highly Amplified Seiche Band (See Fig. 7) as Function of Offshore E_{SWELL}: (a) Barbers Point, Grave Mode; (b) Kahului, Grave Mode; (c) Oceanside, Grave Mode; (d) Barbers Point Higher Mode; (e) Kahului, Higher Mode; (f) Oceanside, Higher Mode
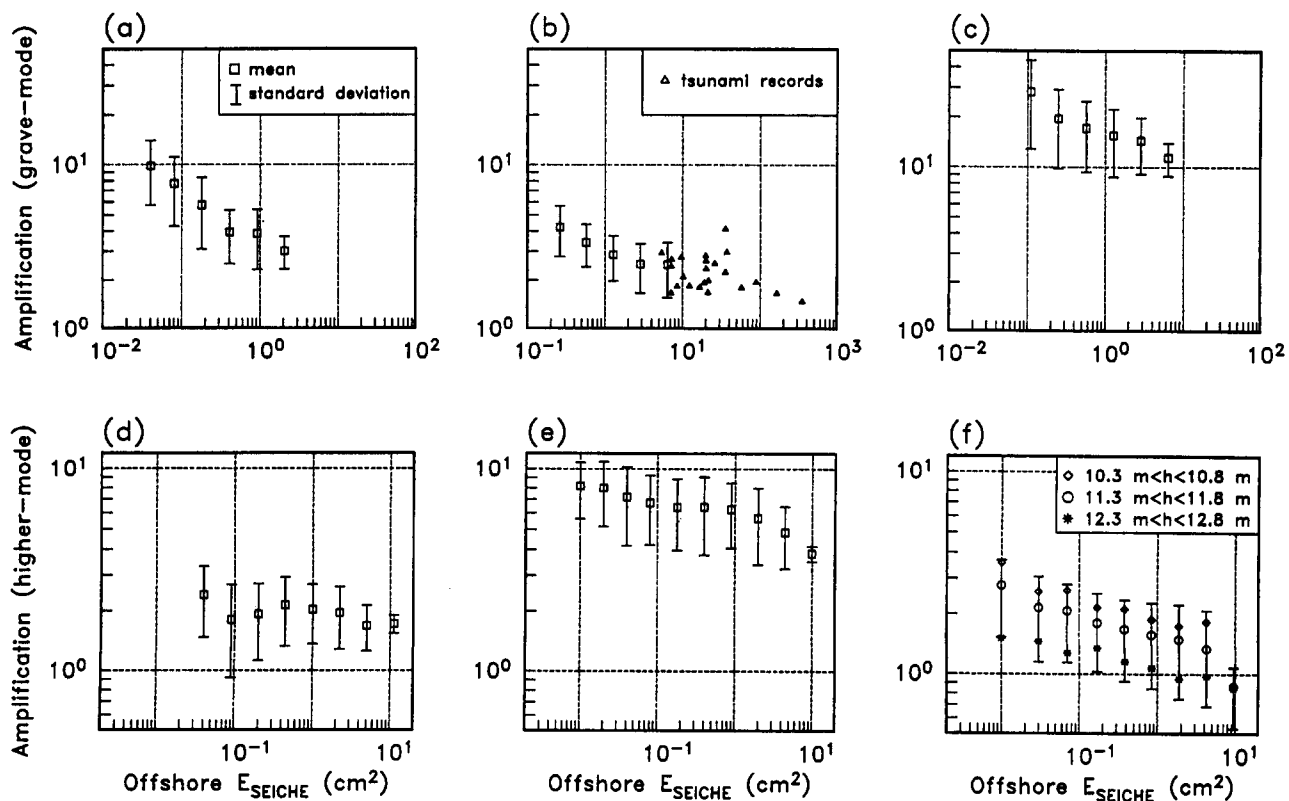

FIG. 9. Ratios of E_{SEICHE} within and Offshore of Harbors at (a–c) Grave Mode and (d–f) next Highly Amplified Seiche Band (See Fig. 7) as Function of Offshore E_{SEICHE}: (a) Barbers Point, Grave Mode; (b) Kahului, Grave Mode; (c) Oceanside, Grave Mode; (d) Barbers Point, Higher Mode; (e) Kahului, Higher Mode; (f) Oceanside, Higher Mode

JOURNAL OF WATERWAY, PORT, COASTAL, AND OCEAN ENGINEERING / SEPTEMBER/OCTOBER 1996 / **237**
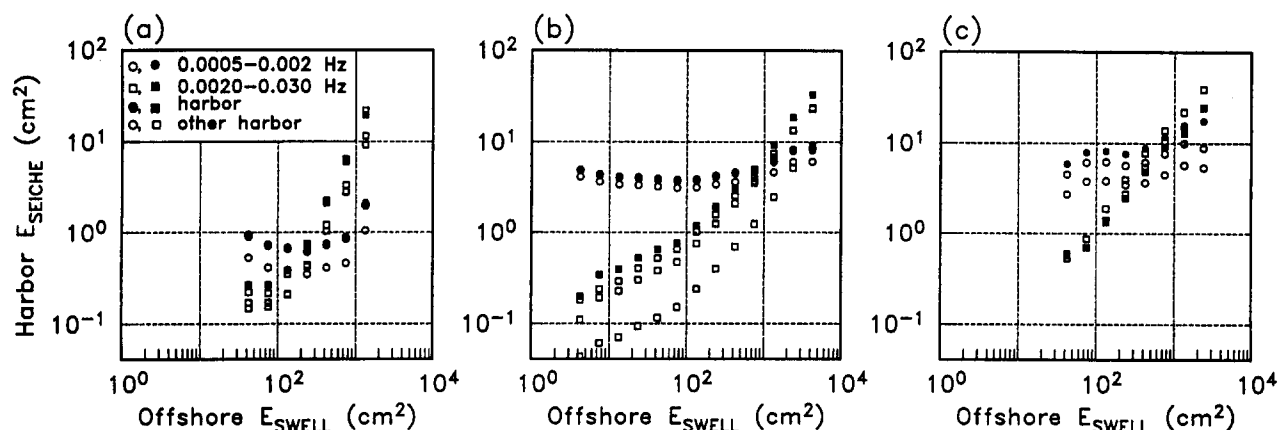
FIG. 10. Mean Energy Integrated over Seiche-Frequency Bands E_{SEICHE} within Each Harbor as Function of Offshore E_{SWELL}: (a) Barbers Point; (b) Kahului; (c) Oceanside

comparable at Kahului and Oceanside and relatively low at Barbers Point (Fig. 10).

SUMMARY

The sources of seiche energy in three small harbors (Fig. 1) are determined by correlating the offshore swell (E_{SWELL}) and seiche (E_{SEICHE}) energies. Below a transition frequency (about 0.001–0.002 Hz), E_{SEICHE} is only weakly correlated to E_{SWELL} [Figs. 2(e–f) and 4(b–c)]. Seiches in this frequency band (which includes the lowest resonant frequency or grave mode) of the harbors are excited by meteorological and other processes, including tsunamis (Fig. 3). When swell energy is low, harbor seiche is largely owing to oscillations in this low-frequency band (Fig. 10). At all three sites, ocean swells are the primary energy source for harbor seiches at frequencies above $\sim$0.002 Hz, as indicated by the high correlation between E_{SWELL} and E_{SEICHE} at these frequencies [Figs. 2(e–f) and 4(d–f)]. Energy levels in this swell-driven frequency band also vary (less dramatically) in response to changes in the swell frequency (i.e., longer swell periods are associated with more seiche energy) (Fig. 5) and with tidal stage (i.e., more energetic at high tide) (Fig. 6). These higher frequency swell-driven seiches are dominant when swell energy levels are high (Fig. 10).

Average energy amplifications (the ratio of harbor to offshore spectra, averaged over all 2.3 h records at each site) vary as a function of seiche frequency and are largest at the grave-mode frequency (Fig. 7). At all three harbors, the average amplification of the grave-mode band decreases (by at least a factor of two) with increasing seiche energy [Figs. 9(a–c)], a trend consistent with nonlinear dissipation mechanisms such as flow separation in the harbor mouth or side wall and bottom friction.

ACKNOWLEDGMENTS

APPENDIX. REFERENCES

Bowers, E. C. (1977). "Harbour resonance due to set-down beneath wave groups." *J. Fluid Mech.*, 79(1), 71–92.
Bowers, E. C. (1992). "Low frequency waves in intermediate depths." *Proc., Int. Coast. Engrg. Conf.*, 23rd, ASCE, New York, N.Y., 832–845.
Elgar, S., Herbers, T. H. C., Okihiro, M., Oltman-Shay, J., and Guza, R. T. (1992). "Observations of infragravity waves." *J. Geophys. Res.*, 97(C10), 15,573–15,577.
Elgar, S., Herbers, T. H. C., and Guza, R. T. (1994). "Reflection of ocean surface gravity waves from a natural beach." *J. Phys. Oceanography*, 24(7), 1503–1511.
Giese, G. S., Chapman, D. C., Black, P. G., and Fornshell, J. A. (1990). "Causation of large-amplitude coastal seiches on the Caribbean Coast of Puerto Rico." *J. Phys. Oceanography*, 20(9), 1449–1458.
Gomis, D., Monserrat, S., and Tintore, J. (1993). "Pressure-forced seiches of large amplitude in inlets of the Balearic Island." *J. Geophys. Res.*, 98(C8), 14,437–14,445.
Herbers, T. H. C., Elgar, S., and Guza, R. T. (1994). "Infragravity-frequency (0.005–0.05 Hz) motions on the shelf, part I: Forced waves." *J. Phys. Oceanography*, 24(5), 917–927.
Herbers, T. H. C., Elgar, S., Guza, R. T., and O'Reilly, W. C. (1995a). "Infragravity-frequency (0.005–0.05 Hz) motions on the shelf, part II: Free waves." *J. Phys. Oceanography*, 25(6), 1063–1079.
Herbers, T. H. C., Elgar, S., and Guza, R. T. (1995b). "Generation and propagation of infragravity waves." *J. Geophys. Res.*, 100(C12), 24863–24872.
Ito, Y. (1970). "On the effect of tsunami-breakwater." *Coast. Engrg. Japan*, 13, 89–102.
Kostense, J. K., Meijer, K. L., Dingemans, M. W., Mynett, A. E., and vah den Bosch, P. (1986). "Wave energy dissipation in arbitrary shaped harbours of variable depth." *Proc., Int. Coast. Engrg. Conf.*, 20th, 2002–2016.
Mei, C. C., and Agnon, Y. (1989). "Long-period oscillations in a harbour induced by incident short waves." *J. Fluid Mech.*, 208, 595–608.
Middleton, J. H., Cahill, M. L., and Hsieh, W. W. (1987). "Edge waves on the Sydney coast." *J. Geophys. Res.*, 92(C9), 9487–9493.
Munk, W. H. (1949). "Surf beats." *Eos Trans. AGU*, 30(6), 849–854.
Munk, W. H., Snodgrass, F., and Carrier, G. (1956). "Edge waves on the continental shelf." *Sci.*, 123(3187), 127–132.
Murakami, H., and Noguchi, E. (1977). "Effects of entrance loss on wave-induced oscillations in rectangular harbor." *Coast. Engrg. Japan*, 20, 27–42.
Nelson, R. C., Treloar, P. D., and Lawson, N. V. (1988). "The dependency of inshore long waves on the characteristics of offshore short waves." *Coast. Engrg.*, 12(3), 213–231.
Okihiro, M., Guza, R. T., and Seymour, R. J. (1992). "Bound infragravity waves." *J. Geophys. Res.*, 97(C7), 11,453–11,469.
Okihiro, M., Guza, R. T., and Seymour, R. J. (1993). "Excitation of seiche observed in a small harbor." *J. Geophys. Res.*, 98(C10), 18,201–18,211.
Okihiro, M., and Guza, R. T. (1995). "Infragravity energy modulation by tides." *J. Geophys. Res.*, 100(C8), 16,143–16,148.
Unluata, U., and Mei, C. C. (1975). "Effects of entrance loss on harbor oscillation." *J. Wtrwy., Harb., Coast. Engrg. Div.*, ASCE, 101(2), 161–180.
Wilson, B. W. (1971). "Tsunami-responses of San Pedro Bay and shelf." *Calif. J. Wtrwy. Harb., Coast. Engrg. Div.*, ASCE, 97(2), 239–258.
Wu, J.-K., and Liu, P. L.-F. (1990). "Harbour excitations by incident wave groups." *J. Fluid Mech.*, 217, 595–613.